Solving the radial part of the time-independent Schrödinger equation for central potentials using Numerov's method. The hydrogen atom.

Reinaldo Magallanes Saunders*

October 2020

1 Introduction

The main objective of this assignment is to approximate solutions to the radial part of the time-independent Schrödinger equation for bound states in the hydrogen atom and to verify the presence of degeneracy in the solutions. Then, the potential with be slightly modified to verify that the degeneracy disappears. This will be done using a script in Python that implements Numerov's algorithm, tailored for this particular problem.

2 Statement of the Problem

For a particle of mass m_p under a central potential $V(r)$, where r is the distance from a fixed center, the Schrödinger equation takes the form:

$$\left[-\frac{\hbar^2}{2m_p}\nabla^2 + V(r)\right]\Psi(\mathbf{r}) = E\Psi(\mathbf{r}) \quad where \quad -\frac{\hbar^2}{2m_p}\nabla^2 + V(r) = H \tag{1}$$

Using spherical coordinates (r, θ, ϕ), where θ is the polar angle and ϕ is the azimuthal angle, the Hamiltonian can be written as

$$H = -\frac{\hbar^2}{2m_p}\frac{1}{r^2}\frac{\partial}{\partial r}\left[r^2\frac{\partial}{\partial r}\right] + \frac{L^2}{2m_p r^2} + V(r) \tag{2}$$

where L^2 is the square of the angular momentum vector operator $\mathbf{L}$:

$$\mathbf{L} = -i\hbar\mathbf{r}\times\nabla \quad and \quad L^2 = -\hbar^2\left[\frac{1}{\sin\theta}\frac{\partial}{\partial\theta}\left(\sin\theta\frac{\partial}{\partial\theta}\right) + \frac{1}{\sin^2\theta}\frac{\partial^2}{\partial\phi^2}\right] \tag{3}$$

Using separation of variables, where we assume $\Psi(r, \theta, \phi) = R(r)Y(\theta, \phi)$, the Schrödinger equation can be split into an angular and a radial equation. The solutions to the angular

*e-mail: rei.magallanes@gmail.com

equation are the spherical harmonics, which are eigenfunctions of L^2 and the z component of the angular momentum L_z:

$$\begin{aligned} L^2 Y_{lm}(\theta,\phi) &= l(l+1)\hbar^2 Y_{lm}(\theta,\phi) \qquad where \quad l \geq 0 \\ L_z Y_{lm}(\theta,\phi) &= m\hbar Y_{lm}(\theta,\phi) \qquad\quad and \quad -l \leq m \leq l \end{aligned} \tag{4}$$

Then, the radial equation is:

$$-\frac{\hbar^2}{2m_p}\frac{1}{r^2}\frac{\partial}{\partial r}\left(r^2\frac{\partial R_{nl}}{\partial r}\right) + \left[V(r) + \frac{\hbar^2 l(l+1)}{2m_p r^2}\right] R_{nl} = E_{nl} R_{nl} \tag{5}$$

The index n arises because, for a given l, we expect a quantization of the bound states. Also, the energy E_{nl} does not depend on m. Introducing the auxiliary function $\chi_{nl}(r) = rR_{nl}(r)$, equation (5) becomes:

$$-\frac{\hbar^2}{2m_p}\frac{d^2\chi_{nl}}{dr^2} + \left[V(r) + \frac{\hbar^2 l(l+1)}{2m_p r^2} - E_{nl}\right]\chi_{nl}(r) = 0 \tag{6}$$

With $\chi_{nl}(r)$ we find that the probability to find the particle at a distance between r and $r+dr$ from the center is $|\,\chi_{nl}(r)|^2$. Thus, if $\chi_{nl}(r)$ is normalized, it can be seen as the radial probability density.

The potential we will consider is the Coulomb potential, which is given by:

$$V(r) = -\frac{Z}{4\pi\varepsilon_0}\frac{e^2}{r} \tag{7}$$

where e is the electron charge, Z is the atomic number and ε_0 is the permittivity of free space. So, instead of the mass of any particle m_p, we consider m_e, the mass of the electron.

For the potential given by equation (7), equation (6) can be solved exactly[1]. Solutions exist for these values of E:

$$E_{nl} = -\frac{m_e e^4}{2(4\pi\varepsilon_0)^2\hbar^2}\frac{Z^2}{n^2} \quad where \quad n \geq l+1 \tag{8}$$

Looking at equation (8) we can see that we have a degeneracy on the energy levels with the same n and different l, addition to the one due to the $2l+1$ possible values for m. Thus, for a given n we have a total degeneracy of n^2.

With these eigenvalues, the solutions to equation (6) are given by[1][2][3]:

$$\chi_{nl}(r) = \sqrt{\left(\frac{2Z}{a_0 n}\right)^3 \frac{(n-l-1)!}{2n(n+l)!}}\rho^{l+1}e^{\frac{-\rho}{2}}L_{n-1-1}^{(2l+1)}(\rho) \quad where \quad \rho = \frac{2Z}{n}\frac{r}{a_0} = 2\sqrt{-\frac{2m_e E_{nl}}{\hbar^2}}r \tag{9}$$

Here, a_0 is the Bohr radius and $L_n^{(\alpha)}(z)$ are the associated Laguerre polynomials[3], which are given by:

$$L_n^{(\alpha)}(z) = \frac{z^{-\alpha}e^z}{n!}\frac{d^n}{dz^n}\left(z^{n+\alpha}e^{-z}\right) \tag{10}$$

The coefficient for $\chi_{nl}(r)$ was chosen so that the wave-functions, which are solutions of equation (1), are orthonormal.

3 Algorithm and Implementation

First, it should be noted that from now on, Rydberg atomic units will be used. This means the following:

$$\hbar = 2m_e = e^2/2 = 1 \quad and \quad 4\pi\varepsilon_0 = 1 \tag{11}$$

This means that the Bohr radius a_0 is 1 and energies are in Ry. In particular, for the hydrogen atom ($Z = 1$), the ground state energy is -1Ry.

Our Schrödinger equation (6) and the Coulomb potential (7) in Rydberg atomic units take the form

$$-\frac{d^2\chi_{nl}}{dr^2} + \left[V(r) + \frac{l(l+1)}{r^2} - E_{nl}\right]\chi_{nl}(r) = 0 \quad and \quad V(r) = -\frac{2Z}{r} \tag{12}$$

while the solutions, (8) and (9), are:

$$E_{nl} = -\frac{Z^2}{n^2} \quad and \quad \chi_{nl}(r) = \sqrt{\left(\frac{2Z}{n}\right)^3 \frac{(n-l-1)!}{2n(n+l)!}}\rho^{l+1}e^{\frac{-\rho}{2}}L_{n-l-1}^{(2l+1)}(\rho) \quad where \quad \rho = \frac{2Z}{n}r \tag{13}$$

Now, Numerov's method is used to integrate second-order differential equations, with suitable initial conditions, of the general form:

$$\frac{d^2y}{dx^2} = -g(x)y(x) + s(x) \quad , \quad y(x_0) = y_0 \quad , \quad y'(x_0) = y_0'. \tag{14}$$

When $s(x) = 0$ and a suitable grid is introduced, Numerov's formula can be written as:

$$y_{n+1} = \frac{(12 - 10f_n)y_n - y_{n-1}f_{n-1}}{f_{n+1}} \quad where \quad f_n = 1 + g_n\frac{(\Delta x)^2}{12} \tag{15}$$

where Δx is the step of the grid.

This implies, comparing with equation (12) that we have to know the value of E_{nl} beforehand. The algorithm actually estimates the energy and improves that estimation by performing checks. The first check is that the classical inversion point, that is, the point κ where $V(\kappa) = E$, falls within the boundaries of the grid. The second is by checking the number of nodes the function has. Since the solution has a polynomial of degree $n - l - 1$, the number of nodes of the calculated function can be compared with this number to check whether the energy estimate is acceptable.

To avoid divergences at large values of the grid, two integrations will be done, one forwards from the origin and one backwards from the end of the interval. This will give two functions over two different parts of the grid. The matching point is chosen to be the classical inversion point. Also, if we want a physical solution, we have the condition that this two functions match with continuous first derivative. It will also be necessary to re-scale them, so that the whole function is normalized.

Finally, we have the problem that equation (12) has a singularity at $r = 0$. To avoid this, we will work with a variable-step grid. A new integration variable x is introduced with

a constant step. If we define $x = x(r)$ then the relation between the constant step Δx and the variable-step grid spacing is given by $\Delta x = x'(r)\Delta r$. We choose:

$$x(r) = \ln \frac{Zr}{a_0} \tag{16}$$

The Bohr radius is there so as to make x dimensionless. Then:

$$\Delta x = \frac{\Delta r}{r} \tag{17}$$

Thus, we have a logarithmic grid over r, and a constant grid over x.

A problem with this grid arises from the fact that, when writing equation (12) in terms of x, a term with χ'_{nl} appears, so we can't use Numerov's method. This can be avoided by defining the following transformation:

$$y_{nl}(x) = \frac{1}{\sqrt{r}}\chi_{nl}(r(x)) \tag{18}$$

With this in mind, equation (12) becomes:

$$\frac{d^2 y_{nl}}{dx^2} + \left[r^2(x)(E_{nl} - V(r(x))) - \left(l + \frac{1}{2}\right)^2 \right] y_{nl}(r(x)) = 0 \quad where \quad V(r(x)) = -\frac{2Z}{r(x)} \tag{19}$$

This no longer presents a singularity for $r = 0$, it's in the form of equation (14) with $s(x) = 0$ and therefore can be solved by Numerov's method.

The upper and lower bounds chosen for the grid are:

$$x_{min} = -8 \quad and \quad r_{max} = 100 \tag{20}$$

The grid doesn't include $r = 0$, which would be for $x \to -\infty$. The step chosen was $\Delta x = 0.01$. This was chosen because this value gives an adequate number of sampling points where the radial function is non-vanishing.

To start the forwards and backwards integration, known behaviour for physical solutions will be taken into account. This is[2]:

$$\begin{aligned} \chi_{nl}(r) &\sim r^{l+1} && for \quad r \to 0 \\ \chi_{nl}(r) &\sim e^{-\sqrt{-E_{nl}}r} && for \quad r \to \infty \end{aligned} \tag{21}$$

which follows from equation (12).

4 Results

In our case, we took the Coulomb potential for the hydrogen atom, which we get, for $V(r)$ with $Z = 1$ in equation (12). It is shown, near the origin, in Figure 1.

Solutions were obtained for $n = 1, 2, 3$, to compare with exact results. These can be seen in Figures 2 through 7.

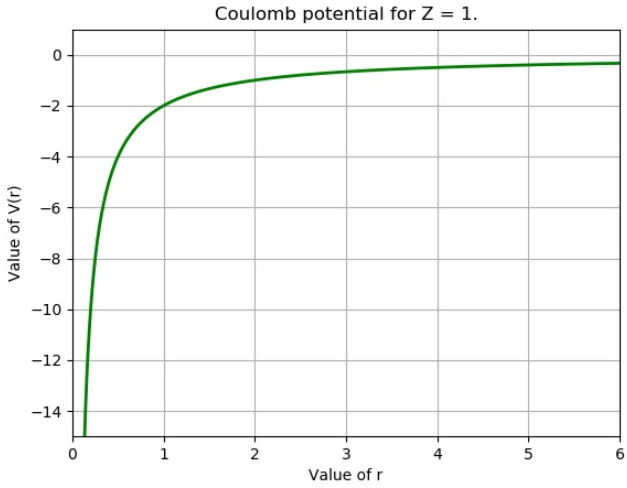

Figure 1: Coulomb potential for the hydrogen atom.

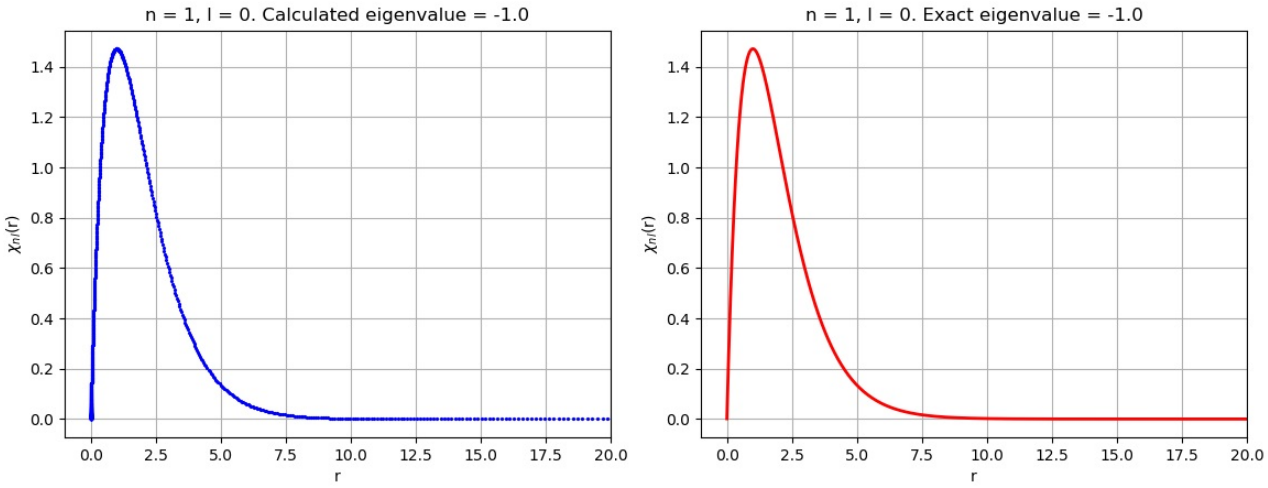

Figure 2: Solution of (12) for $Z = 1$ with $n = 1$ and $l = 0$. Left: solution obtained. Right: exact solution.

For each value of n we get n different χ_{nl} functions, since they can be seen as radial probability densities and we are not taking into account angular related functions. The graphs are not shown over the whole grid, since showing the whole grid wouldn't add anything visually; functions were vanishingly small, or zero, over the remainder of the grid.

We can see that in every case the solutions obtained with the algorithm are exactly the same as the exact solutions given by equation (13). Furthermore, the eigenvalues match as well, both calculated and exact values are the same.

To appreciate the limits of the chosen grid, solutions for $l = 0$, with increasing value of n where calculated and plotted. These can be seen in Figures 8 through 10.

As we can see, it is when we get to $n = 6$ when the grid fails, since it's too small. We note that the functions here don't quite match in the upper bound of the grid. This is because the algorithm forces the calculated solution to go towards zero at the end of the grid. This can be easily fixed with a bigger grid. Even though it falls short for $n = 6$, we can see that the

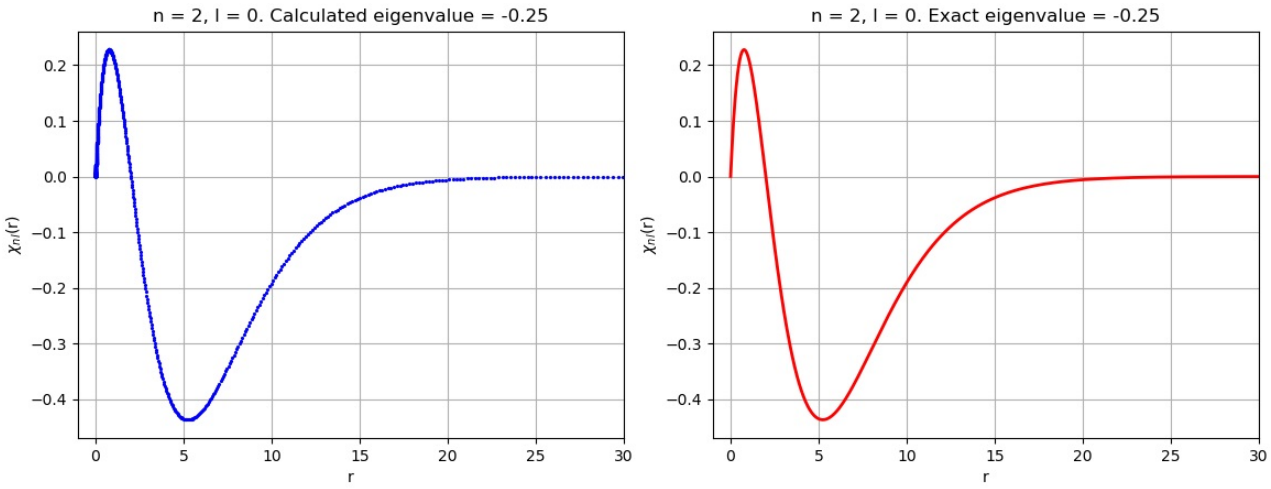

Figure 3: Solution of (12) for $Z = 1$ with $n = 2$ and $l = 0$. Left: solution obtained. Right: exact solution.

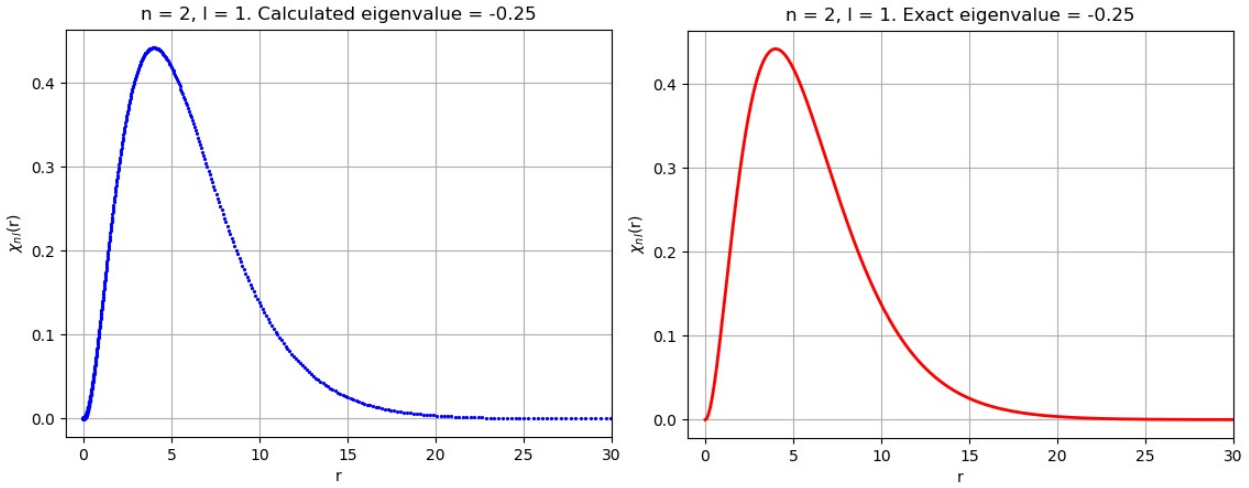

Figure 4: Solution of (12) for $Z = 1$ with $n = 2$ and $l = 1$. Left: solution obtained. Right: exact solution.

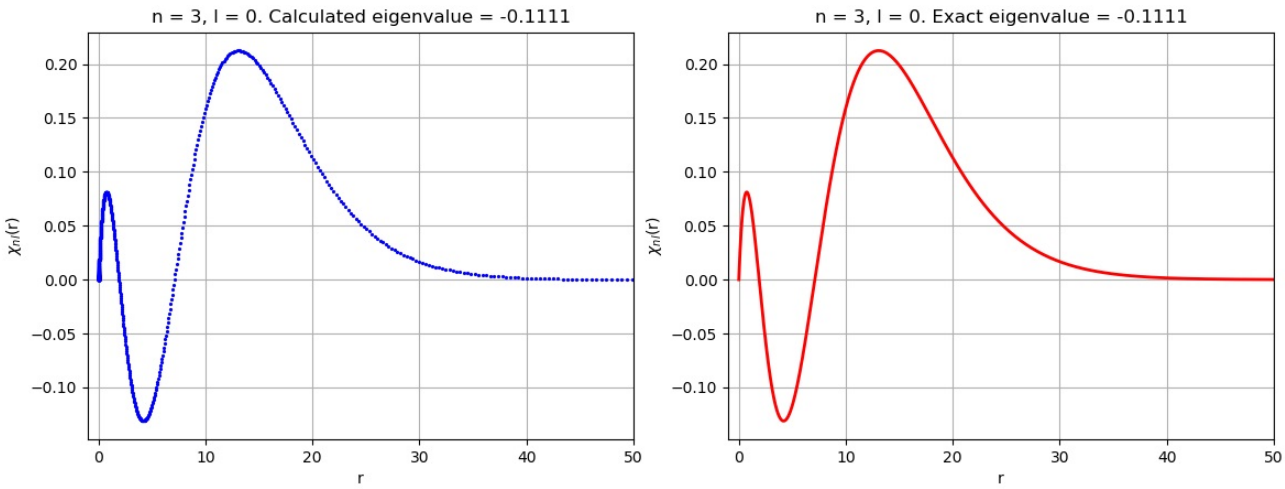

Figure 5: Solution of (12) for $Z = 1$ with $n = 3$ and $l = 0$. Left: solution obtained. Right: exact solution.

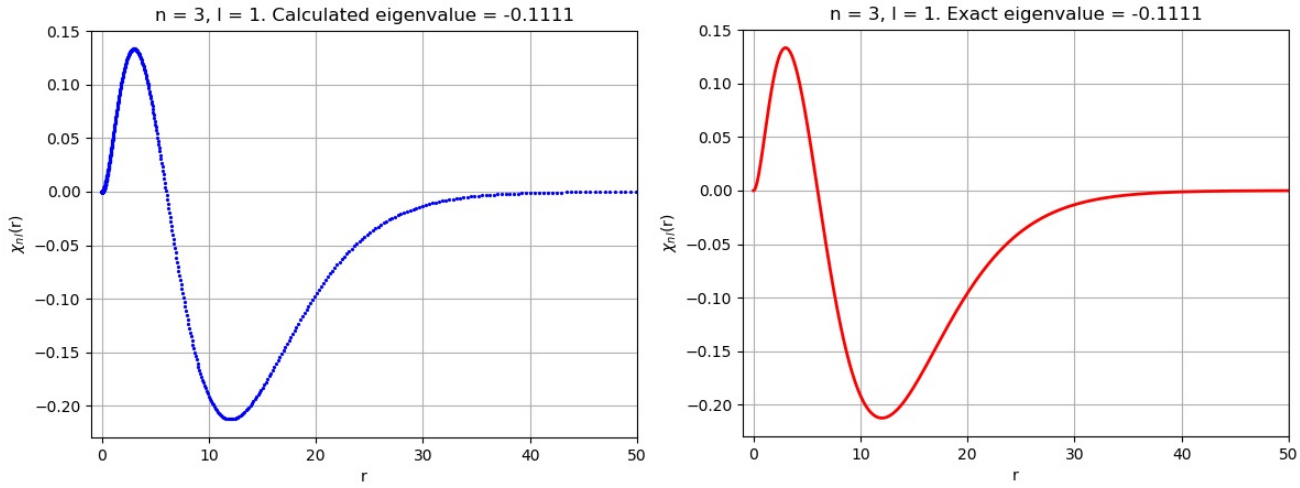

Figure 6: Solution of (12) for $Z = 1$ with $n = 3$ and $l = 1$. Left: solution obtained. Right: exact solution.

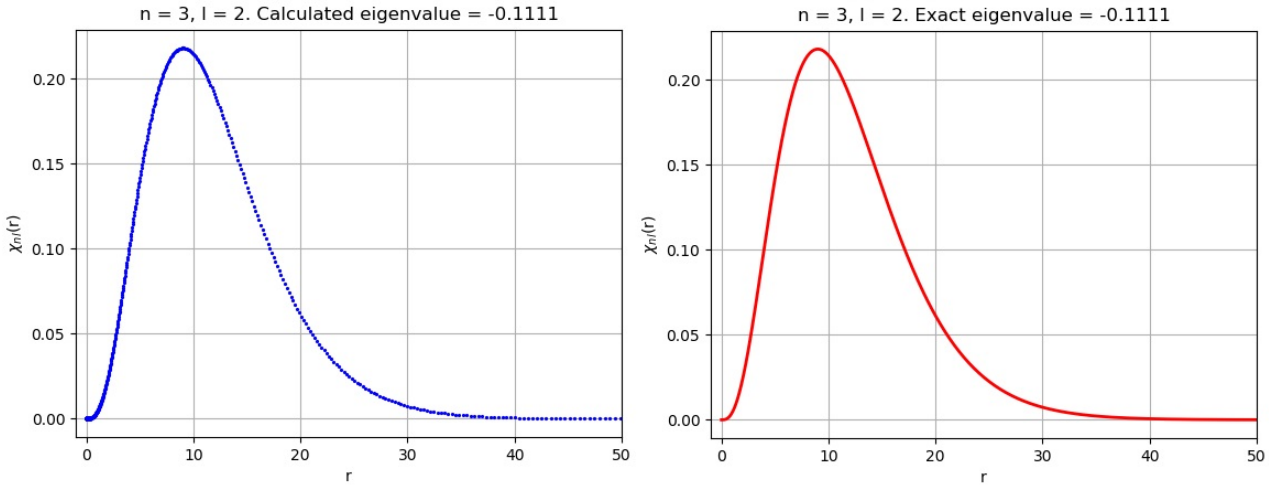

Figure 7: Solution of (12) for $Z = 1$ with $n = 3$ and $l = 2$. Left: solution obtained. Right: exact solution.

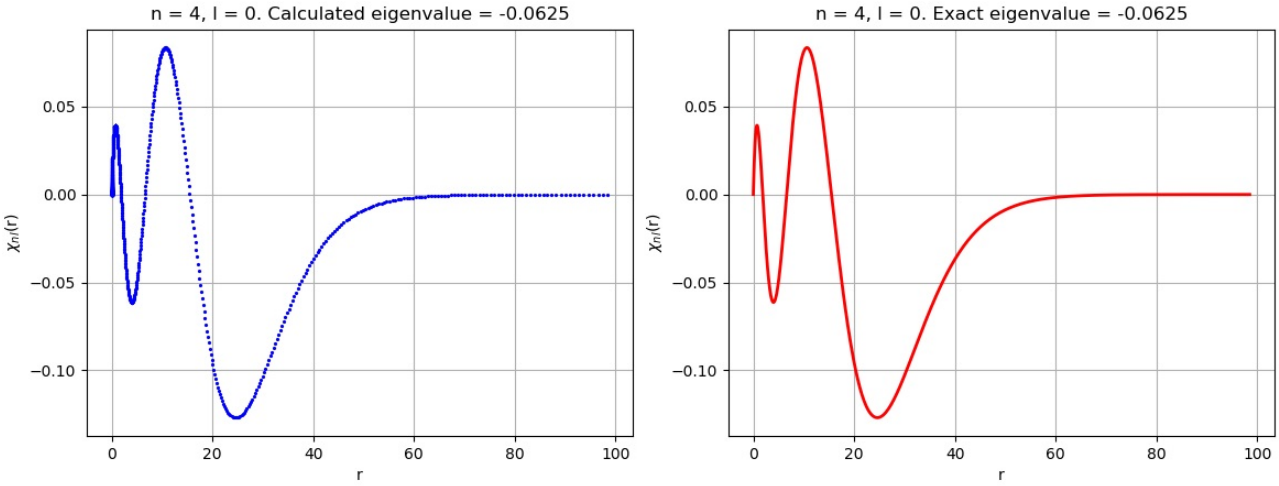

Figure 8: Solution of (12) for $Z = 1$ with $n = 4$ and $l = 0$. Left: solution obtained. Right: exact solution.

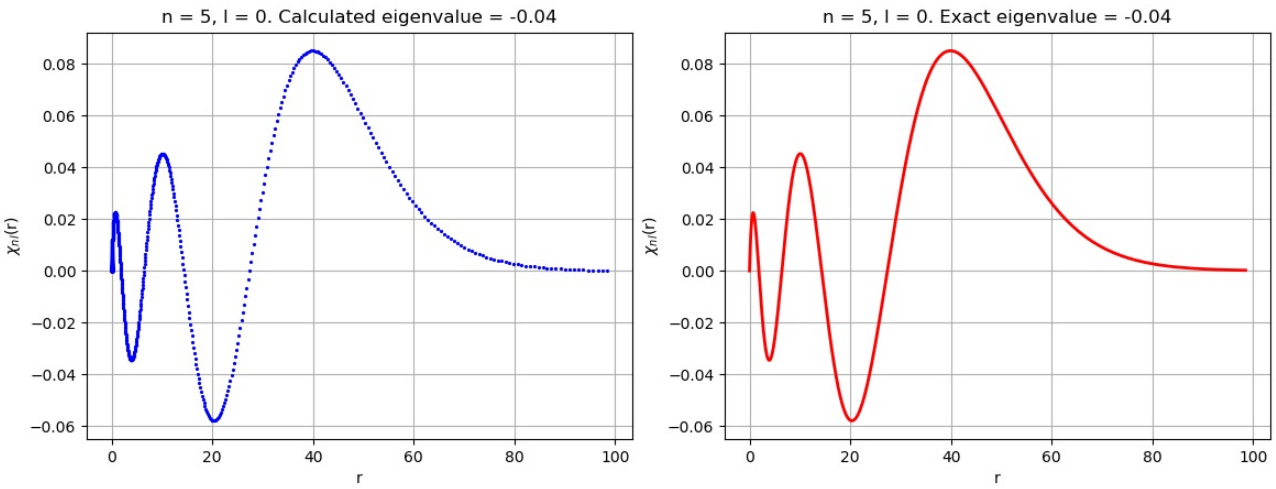

Figure 9: Solution of (12) for $Z = 1$ with $n = 5$ and $l = 0$. Left: solution obtained. Right: exact solution.

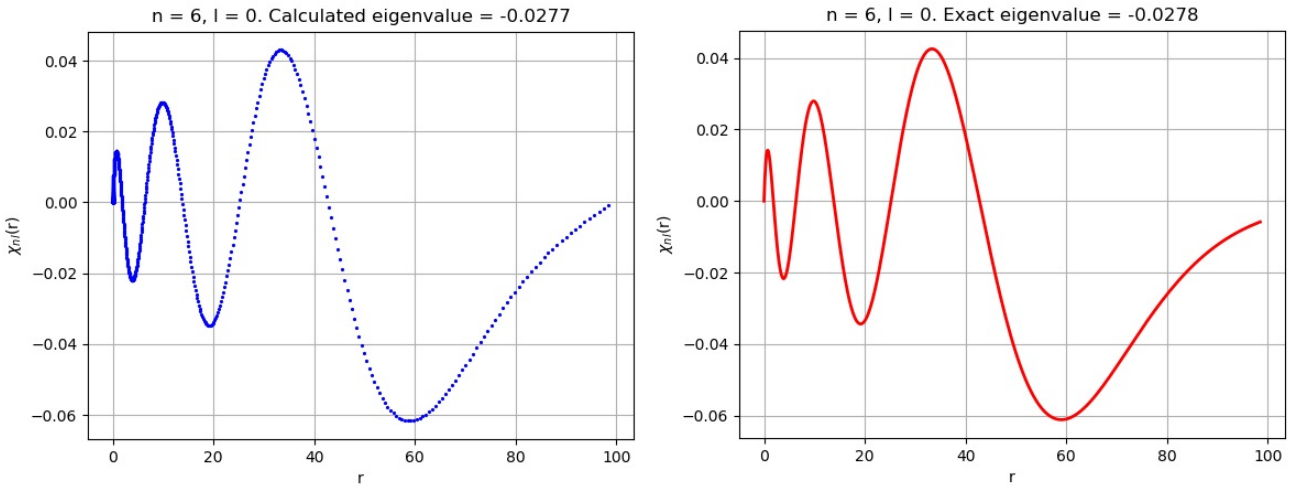

Figure 10: Solution of (12) for $Z = 1$ with $n = 6$ and $l = 0$. Left: solution obtained. Right: exact solution.

obtained solutions still are the same as the exact solutions. Also, the eigenvalues obtained still match the exact ones. It is for $n = 6$ that we start to see a discrepancy, however small. In fact, number shown in the Figure is a product of how the *round* function works in Python. The exact eigenvalue is $-0.02\overline{7}$ while the calculated eigenvalue was -0.0277331. This is the only one with a discrepancy of this kind. The other ones where correct to at least 7 digits.

We can see the presence of degeneracy. For instance, in Figures 5, 6 and 7, we see that we get three different solutions for the same eigenvalue.

With these results, we can compare the expectation values of r and r^{-1} obtained with these solutions with theoretical results. We know[5] that for the wave function of the hydrogen atom ψ_{nlm} with $a_0 = 1$:

$$\langle\psi_{nlm}|r|\psi_{nlm}\rangle = \frac{3n^2 - l(l+1)}{2} \quad and \quad \langle\psi_{nlm}|\frac{1}{r}|\psi_{nlm}\rangle = \frac{1}{n^2} \tag{22}$$

Thus, since the spherical harmonics are orthonormal over the solid angle and from (13) $\rho = 2r/n$, we get:

$$\langle\psi_{nlm}|r|\psi_{nlm}\rangle = \frac{n^2}{4}\int_0^\infty r dr \chi_{nl}^2(r) = \frac{3n^2 - l(l+1)}{2} \tag{23}$$

and

$$\langle\psi_{nlm}|\frac{1}{r}|\psi_{nlm}\rangle = \frac{n^2}{4}\int_0^\infty dr \frac{\chi_{nl}^2(r)}{r} = \frac{1}{n^2} \tag{24}$$

Results can be seen in Table 1. Results were truncated and are shown with 7 significant figures.

n	l	$\langle r\rangle$ calculated	theoretical $\langle r\rangle$	$\langle r^{-1}\rangle$ calculated	theoretical $\langle r^{-1}\rangle$
1	0	1.500024	1.5	1.000016	1
2	0	6.000099	6	0.2500041	0.25
2	1	5.000083	5	0.2500041	0.25
3	0	13.50022	13.5	0.1111129	$0.\overline{1}$
3	1	12.50020	12.5	0.1111129	$0.\overline{1}$
3	2	10.50017	10.5	0.1111129	$0.\overline{1}$
4	0	24.00039	24	0.06250103	0.0625
5	0	37.49953	37.5	0.04000152	0.04
6	0	53.39278	54	0.02812086	$0.02\overline{7}$

Table 1: Expectation values of r and r^{-1}.

It can be seen that results are as good as can be expected, except for $n = 6$ and $l = 0$. This is because, looking at Figure 10, we can see that the algorithm forces the radial function to go towards zero faster than it needs to. This can be fixed by taking a bigger interval.

One thing one might wonder, is how the radial wave function changes with the atomic number Z. From (13) we can see clearly that the energy is a quadratic in Z for a given n,

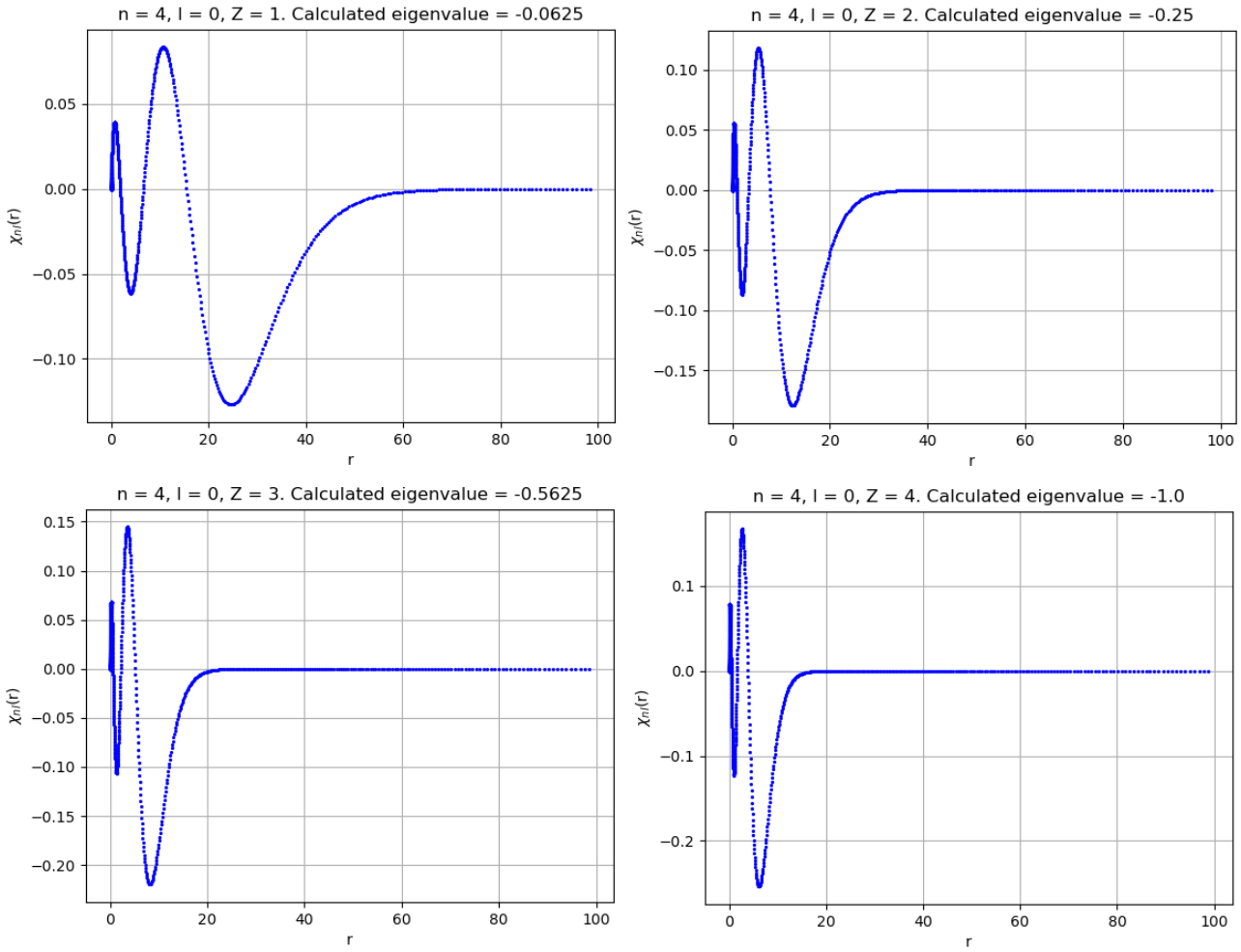

Figure 11: Solutions of (12) for $Z = 1, 2, 3, 4$ with $n = 4$ and $l = 0$.

but it's not that easy to see at first glance how $\chi_{nl}(r)$ changes as Z does. So, we took fixed values for n and l, namely $n = 4$ and $l = 0$, to see how the graphs in Figure 8 change.

Results can be seen in Figure 11. We can see that indeed the energy changes as a quadratic in Z. We can also see that, as Z increases, the interval where the function is vanishingly small gets smaller while the peaks grow. This makes sense since increasing Z means a stronger potential and thus a higher probability of finding the electron near the origin.

5 Perturbation of Potential

For a value of n, we will get n different solutions with the same eigenvalue, given by the different possible values of l. We will modify slightly the potential and see that this n-fold degeneracy disappears.

We will take a new potential of the form

$$V_{new}(r) = \frac{-2}{r} + \frac{\epsilon}{r^2} \tag{25}$$

where ϵ is a small number. We will see how the energies change for a particular value of $\epsilon = 1 \times 10^{-4}$ and, for $n = 3$, we will see how the energies change as functions of ϵ for all possible values of l.

To get an expression for the eigenvalue of the new system with potential given by equation (25) we will apply perturbation theory to the system with potential given by (12) to get a first-order correction to the energy.

First, we will write the Hamiltonian of the new system $\hat{H}$ as the sum of the Hamiltonian of the unperturbed system $\hat{H}_0$, given by equation (1), and a perturbation $\hat{H}_p$. Then:

$$\hat{H} = \hat{H}_0 + \hat{H}_p \quad where \quad H_0 = \nabla^2 - \frac{2}{r} \quad and \quad H_p = \frac{\epsilon}{r^2} \tag{26}$$

It follows[5] that the n-fold degenerate level E_{nl} of the unperturbed problem will split into n different levels E_{n_α}, such that:

$$E_{n_\alpha} = E_{nl} + \xi_{n_\alpha} \quad for \quad \alpha = 0, 1, ..., n-1 \tag{27}$$

where, for each n-fold degenerate level, ξ_{n_α} are given by the eigenvalues of the matrix H_p with entries:

$$[H_p]_{\alpha\beta} = \left\langle \Psi_{n_\alpha} \middle| \hat{H}_p \middle| \Psi_{n_\beta} \right\rangle \tag{28}$$

Here, Ψ_{n_α} are the eigenfunctions of H_0, i.e., solutions to equation (1) with Coulomb potential for $Z = 1$. They are given by[1][3], in Rydberg atomic units:

$$\Psi_{nlm}(r, \theta, \phi) = \sqrt{\left(\frac{2}{n}\right)^3 \frac{(n-l-1)!}{2n(n+l)!}} \rho^l e^{\frac{-\rho}{2}} L_{n-l-1}^{(2l+1)}(\rho) Y_{lm}(\theta, \phi) \quad , \quad \rho = \frac{2}{n} r \tag{29}$$

Therefore:

$$[H_p]_{\alpha\beta} = \Sigma_{\alpha\beta} \int_0^\infty r^2 dr \frac{1}{r^2} e^{-\rho} \rho^{\alpha+\beta} L_{n-\alpha-1}^{(2\alpha+1)}(\rho) L_{n-\beta-1}^{(2\beta+1)}(\rho) \int_\Omega d\Omega Y_{\alpha m}^*(\theta,\phi) Y_{\beta m}(\theta,\phi)$$
$$\Sigma_{\alpha\beta} = \left(\frac{2}{n}\right)^3 \frac{\epsilon}{2n} \sqrt{\frac{(n-\alpha-1)!(n-\beta-1)!}{(n+\alpha)!(n+\beta)!}} \tag{30}$$

where Ω denotes solid angle. Now, the spherical harmonics are orthonormal over the whole solid angle, so, writing the radial integral in terms of ρ:

$$[H_p]_{\alpha\beta} = \epsilon \left(\frac{2}{n}\right)^2 \frac{(n-l-1)!}{2n(n+l)!} \left[\int_0^\infty e^{-\rho} \rho^{2l} \left[L_{n-l-1}^{(2l+1)}(\rho)\right]^2 d\rho\right] \delta_{\alpha\beta} \tag{31}$$

Let's focus on the integral between brackets. First, we are going to use a property[4] of the associated Laguerre polynomials:

$$\sum_{\nu=0}^{j} L_\nu^{(k)}(x) = L_j^{(k+1)}(x) \quad therefore \quad L_{n-l-1}^{(2l+1)}(\rho) = \sum_{\nu=0}^{n-l-1} L_\nu^{(2l)}(\rho) \tag{32}$$

Combining this with the following identity[6]:

$$\left(\sum_{\nu=0}^{N} a_\nu\right)^2 = \sum_{\nu=0}^{N} a_\nu^2 + 2 \sum_{j=1}^{N} \sum_{i=0}^{j-1} a_j a_i \tag{33}$$

we get:

$$\left[L_{n-l-1}^{(2l+1)}(\rho)\right]^2 = \sum_{\nu=0}^{n-l-1} \left[L_\nu^{(2l)}(\rho)\right]^2 + 2 \sum_{j=1}^{n-l-1} \sum_{i=0}^{j-1} L_i^{(2l)}(\rho) L_j^{(2l)}(\rho) \tag{34}$$

Now, since the associated Laguerre polynomials are polynomials of ρ and the summations are finite, we can interchange the integral with the summation, by linearity of the integral.

Then, the integral between brackets in equation (31) becomes

$$\sum_{\nu=0}^{n-l-1} \int_0^\infty e^{-\rho} \rho^{2l} \left[L_\nu^{(2l)}(\rho)\right]^2 d\rho + 2 \sum_{j=1}^{n-l-1} \sum_{i=0}^{j-1} \int_0^\infty e^{-\rho} \rho^{2l} L_i^{(2l)}(\rho) L_j^{(2l)}(\rho) d\rho \tag{35}$$

But the associated Laguerre polynomials are orthogonal over $[0,\infty)$ with that weighting function[4]:

$$\int_0^\infty e^{-x} x^k L_i^k(x) L_j^k(x) dx = \frac{(i+k)!}{i!} \delta_{ij} \tag{36}$$

so the integrals given by the double sum are all zero.

Then, using equation (33), we get:

$$[H_p]_{\alpha\beta} = \epsilon \left(\frac{2}{n}\right)^2 \frac{(n-l-1)!}{2n(n+l)!} \left[\sum_{\nu=0}^{n-l-1} \frac{(\nu+2l)!}{\nu!}\right] \delta_{\alpha\beta} \tag{37}$$

Now, because of the $\delta_{\alpha\beta}$, this is a diagonal matrix. Therefore, it's eigenvalues are just it's entries. Then, the first-order correction for the energy is:

$$E_{n_\alpha} = -\frac{1}{n^2} + \epsilon \left(\frac{2}{n}\right)^2 \frac{(n-l-1)!}{2n(n+l)!} \left[\sum_{\nu=0}^{n-l-1} \frac{(\nu+2l)!}{\nu!}\right] \tag{38}$$
$$\alpha = l = 0, 1, 2, ..., n-1$$

6 Implementation and Results

To get the eigenvalues, the only thing to change is the function that sets up the array for the potential to add the corresponding perturbation. First, we chose $\epsilon = 1 \times 10^{-4}$. So, we have:

$$V_{new} = -\frac{2}{r} + \frac{1 \times 10^{-4}}{r^2} \tag{39}$$

Then, after changing the function that sets up the potential in the code, we add two lines of code to make the algorithm print the obtained eigenvalue, as well as the first-order correction obtained with perturbation theory, given by equation (38).

Results are shown in Table 2. A column with the eigenvalues for the Hydrogen atom was added for comparison.

n	l	Eigenvalue obtained	First-order correction	Hydrogen atom
1	0	-0.999800	-0.99995	-1
2	0	-0.249975021	-0.249975	-0.25
2	1	-0.24999166700	-0.24999166666	
3	0	-0.111103	-0.111094	$-0.\overline{1}$
3	1	-0.11110864	-0.11110555	
3	2	-0.11110962	-0.11110777	
4	0	-0.0624968	-0.0624975	-0.0625
4	1	-0.06249895	-0.06249583	
4	2	-0.06249937	-0.0624975	
4	3	-0.06249955	-0.06249821	

Table 2: Eigenvalues for potential given by equation (39).

The values are shown up to the three decimal places where the first-order correction differs from the eigenvalue obtained with the algorithm. If the correction has less decimal places than the eigenvalue obtained, it's because that's the exact number. Numbers were truncated, not rounded.

Finally, to see how the eigenvalues change as a function of ϵ, in equation (22), $n = 3$ was taken, and the energies obtained, for $l = 0, 1, 2.$, with the algorithm for different values of ϵ were plotted. This can be seen in Figure 12.

At first glance, it may seem like the eigenvalues are linear with respect to ϵ. But if we look closely, we can see this is not the case.

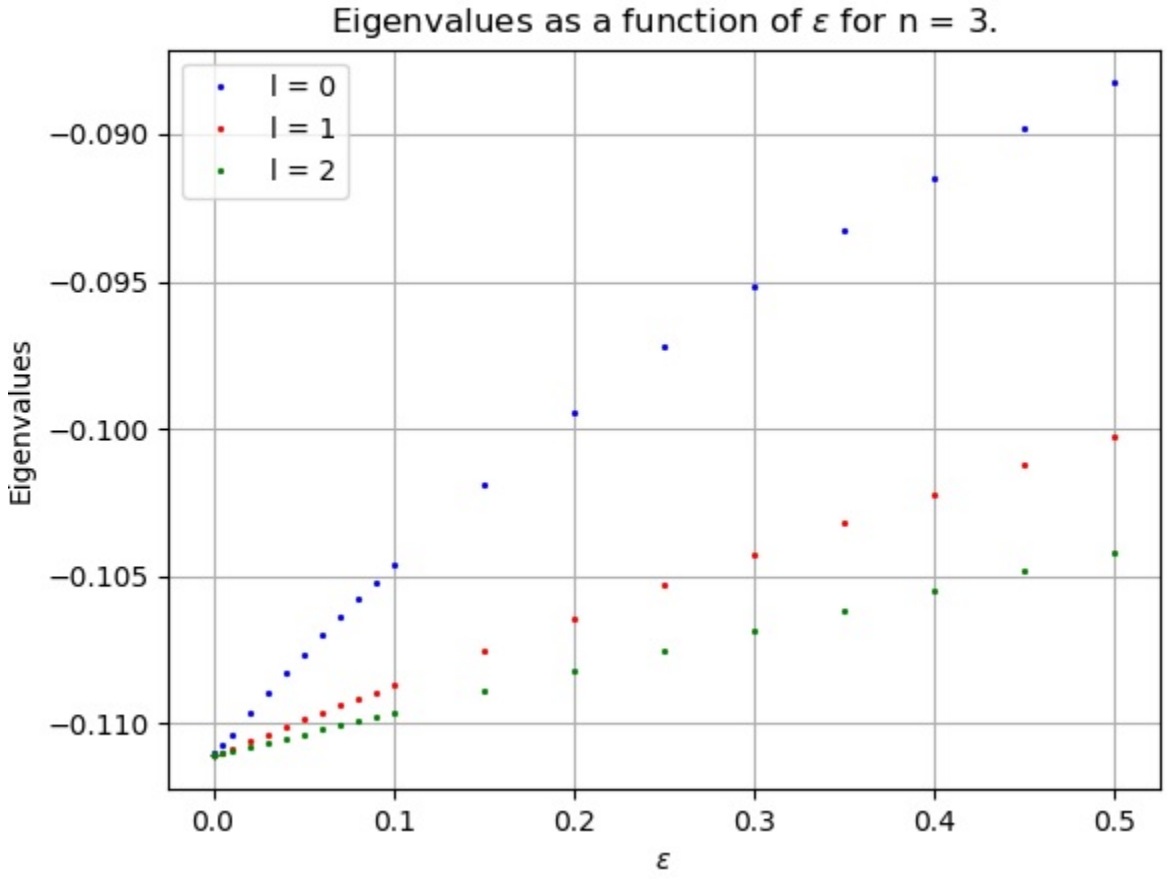

Figure 12: Eigenvalues for $n = 3$ as a function of ϵ.

References

[1] Hydrogen atom. (n.d.). In *Wikipedia*. Retrieved September 22, 2019, from https://en.wikipedia.org/wiki/Hydrogen_atom

[2] Giannozzi, P. (2019) "*Numerical Methods in Quantum Mechanics*". Lecture notes. University of Udine, Italy. Academic year 2018/2019.

[3] No Author. (2010) "*The Hydrogen Atom*". Lecture notes. Physics 342. Reed College, Portland, United States of America.

[4] Weisstein, Eric W. (n.d.) "*Associated Laguerre Polynomial*". From MathWorld, A Wolfram Web Resource. Retrieved September 26, 2019, from http://mathworld.wolfram.com/AssociatedLaguerrePolynomial.html

[5] Zettili, N. (2009) "*Quantum Mechanics: Concepts and Applications*". United Kingdom: John Wiley & Sons, Ltd.

[6] Weisstein, Eric W. (n.d.) "*Power Sum*". From MathWorld, A Wolfram Web Resource. Retrieved September 28, 2019, from http://mathworld.wolfram.com/PowerSum.html